Space Vector Modulation of a Nine-Phase Voltage Source Inverter

Gabriele Grandi, Giovanni Serra, and AngeloTani
Dipartimento di Ingegneria Elettrica
Alma Mater Studiorum - Università di Bologna
Viale Risorgimento, 2 – 40136, Bologna (IT)
Email: *name.surname*@mail.ing.unibo.it

***Abstract*—A generalized multi-phase space vector theory is considered for developing the space vector modulation of a nine-phase voltage source inverter (VSI). The space vector modulation (SVM) is based on the control of the voltage vector in the first *d-q* plane, imposing to be zero the voltage vectors in second, third, and fourth *d-q* planes, as in the relevant case of balanced sinusoidal load voltages. The proposed switching pattern includes one-leg commutation at a time, with the possibility to share the zero voltage between the two null vectors. The modulation limits are analytically determined. In particular, it is shown that the maximum modulation index coincides with the theoretical value obtained in the case of sinusoidal balanced waveforms of a nine-phase VSI, proving that the proposed SVM strategy allows full dc bus voltage utilization. The analysis is confirmed by a complete set of numerical simulations.**

I. Introduction

Multi-phase motor drives have many advantages over traditional three-phase motor drives such as reducing the amplitude and increasing the frequency of torque pulsations, reducing the rotor harmonic current losses and lowering the dc link current harmonics. In addition, owing to their redundant structure, multi-phase motor drives improve the system reliability. As a consequence, the use of multi-phase inverters together with multi-phase ac machines has been recognized as a viable approach to obtain high power ratings with current limited devices [1]-[2].

Among the various possible number of phases, the multiples of three present some advantages, such as the possibility to build the multi-phase inverter as an hardware combination of standard three-phase VSIs, having proved reliability and effective protection circuitry. Furthermore, the stator core laminations of the ac machine has a number of slot multiple of three, offering the possibility to realize the multi-phase stator core with minimum adjustment with respect to standard machines.

In alternative to the traditional carrier-based PWM [3], [4], the multiple space vector approach can be adopted to determine the firing signal for the power switches of a multi-phase VSI, introducing the multi-phase space vector modulation (SVM) techniques [5]-[8]. In fact, an extension of the well-known space vector theory can be still employed to represent the behavior of multi-phase systems, leading to an elegant and effective vector approach in multiple *d-q* planes [9].

Nowadays, nine-phase inverters (see Fig. 1) have been already studied in [10], [11]. However, an explicit SVM algorithm for nine-phase VSI has not been presented yet.

In this paper a SVM technique based on the multiple space vector concept applied to a nine-phase VSI is presented in details. In particular, the aim of the authors is to extend the space vector modulation for seven-phase VSI presented in [8] to the case of nine-phase VSI, considering reference space vectors in all the four *d-q* planes. The proposed SVM strategy univocally selects the inverter switch configurations among the $2^9 = 512$ possibilities by privileging the space vector on the first *d-q* plane, d_1-q_1, the one responsible for balanced sinusoidal output voltage waveforms of the first sequence. This selection is based on the definition of 18 symmetric sectors on the d_1-q_1 plane.

The resulting switching patterns, collected in a general switching table, include eight active and two null configurations, with a single leg commutation for each configuration change. The application times of active vectors are expressed in terms of duty cycles on the basis of a detailed analytical approach, whereas the application time of the null vector is arbitrarily shared between the two null configurations.

The modulation limits are given for balanced sinusoidal voltages by introducing the maximum modulation index. A complete set of numerical results confirms the effectiveness of the proposed SVM strategy.

II. Multiple Space Vector Transformation for Nine-Phase Systems

The space vector transformation for a nine-phase system leads to a zero-sequence component and four independent space vectors among the eight available ones [9].

In this paper the following space vectors are adopted to represent the nine-phase system, being $\alpha = exp(j2\pi/9)$:

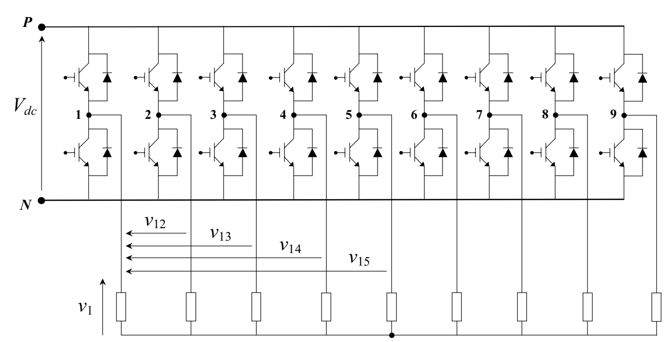

Fig. 1. Scheme of a nine-phase VSI feeding a nine-phase load.

1-4244-0755-9/07/$20.00 ©2007 IEEE

$$
\begin{cases}
x_0 = \dfrac{1}{9}\left[x_1 + x_2 + x_3 + x_4 + x_5 + x_6 + x_7 + x_8 + x_9\right] \\
\overline{x}_1 = \dfrac{2}{9}\left[x_1 + x_2\alpha + x_3\alpha^2 + x_4\alpha^3 + x_5\alpha^4 + x_6\alpha^5 + x_7\alpha^6 + x_8\alpha^7 + x_9\alpha^8\right] \\
\overline{x}_2 = \dfrac{2}{9}\left[x_1 + x_2\alpha^2 + x_3\alpha^4 + x_4\alpha^6 + x_5\alpha^8 + x_6\alpha + x_7\alpha^3 + x_8\alpha^5 + x_9\alpha^7\right] \\
\overline{x}_3 = \dfrac{2}{9}\left[(x_1 + x_4 + x_7) + (x_2 + x_5 + x_8)\alpha^3 + (x_3 + x_6 + x_9)\alpha^6\right] \\
\overline{x}_4 = \dfrac{2}{9}\left[x_1 + x_2\alpha^4 + x_3\alpha^8 + x_4\alpha^3 + x_5\alpha^7 + x_6\alpha^2 + x_7\alpha^6 + x_8\alpha + x_9\alpha^5\right]
\end{cases}
\qquad (1)
$$

Note that the space vector $\overline{x}_3$ has a particular expression since 3 is a factor of the number of phases $n = 9$, which is not a prime.

On the basis of (1), the inverse space vector transformation becomes

$$
x_k = x_0 + \overline{x}_1 \cdot \alpha^{(k-1)} + \overline{x}_2 \cdot \alpha^{2(k-1)} + \overline{x}_3 \cdot \alpha^{3(k-1)} + \overline{x}_4 \cdot \alpha^{4(k-1)} \qquad k = 1, 2, \ldots, 9 \qquad (2)
$$

where the symbol " $\cdot$ " denotes the inner (scalar) product. The four space vectors $\overline{x}_1$, $\overline{x}_2$, $\overline{x}_3$, and $\overline{x}_4$ lie in the planes called d_1-q_1, d_2-q_2, d_3-q_3, and d_4-q_4, corresponding to the sequence 1, 2, 3, and 4, respectively.

III. Nine-Phase Voltage Source Inverters

The scheme of a nine-phase VSI is represented in Fig. 1. The star-connected load is supposed to be balanced, with a single central point 0.

With reference to transformation (1), the zero-sequence component of the load voltages is always zero (balanced load), whereas the multiple space vectors can be written as

$$
\begin{cases}
\overline{v}_1 = \dfrac{2}{9}V_{dc}\left[S_1 + S_2\alpha + S_3\alpha^2 + S_4\alpha^3 + S_5\alpha^4 + S_6\alpha^5 + S_7\alpha^6 + S_8\alpha^7 + S_9\alpha^8\right] \\
\overline{v}_2 = \dfrac{2}{9}V_{dc}\left[S_1 + S_2\alpha^2 + S_3\alpha^4 + S_4\alpha^6 + S_5\alpha^8 + S_6\alpha + S_7\alpha^3 + S_8\alpha^5 + S_9\alpha^7\right] \\
\overline{v}_3 = \dfrac{2}{9}V_{dc}\left[(S_1 + S_4 + S_7) + (S_2 + S_5 + S_8)\alpha^3 + (S_3 + S_6 + S_9)\alpha^6\right] \\
\overline{v}_4 = \dfrac{2}{9}V_{dc}\left[S_1 + S_2\alpha^4 + S_3\alpha^8 + S_4\alpha^3 + S_5\alpha^7 + S_6\alpha^2 + S_7\alpha^6 + S_8\alpha + S_9\alpha^5\right]
\end{cases}
\qquad (3)
$$

where S_k represents the switch state (0, 1) of the k-th inverter leg (k = 1, 2, …, 9). It can be shown that the instantaneous load voltages can be expressed in terms of the switch state as

$$
v_k = V_{dc}\left[S_k - \frac{1}{9}(S_1 + S_2 + S_3 + S_4 + S_5 + S_6 + S_7 + S_8 + S_9)\right]. \qquad (4)
$$

There are 2^9 = 512 possible switch configurations. For the sequences 1, 2, and 4 (i.e., in d_1-q_1, d_2-q_2, and d_4-q_4 planes), the configurations (000000000) and (111111111) correspond to the null vector, whereas the other 510 configurations correspond to different active vectors. For the sequence 3 (i.e., in the d_3-q_3 plane) there are many configurations corresponding to the null vector and many configurations corresponding to each one of the 36 active vectors. The voltage vectors corresponding to all the 512 switch configurations in the four d-q planes are represented by dots in Fig. 2.

IV. Space Vector Modulation

The goal of the space vector modulation for a nine-phase VSI is to generate the four load voltage space vectors ($\overline{v}_1$, $\overline{v}_2$, $\overline{v}_3$, and $\overline{v}_4$) with a given average value within the switching period ($\overline{v}_{1ref}$, $\overline{v}_{2ref}$, $\overline{v}_{3ref}$, and $\overline{v}_{4ref}$), corresponding to the nine line-to-neutral load voltages (v_1, v_2, …, v_9). This condition leads to eight independent scalar constraints that can be univocally satisfied by selecting, in each cycle period, inverter configurations corresponding to eight active and a null voltage vector.

In order to optimize the harmonic content and minimize the current ripple, the eight active configurations should correspond to voltage vectors lying as close as possible to the reference voltage vectors. Since in nine-phase inverters there are four independent reference voltage vectors, a possible configuration selection criterion consists in privileging the voltage vector on the d_1-q_1 plane, $\overline{v}_{1ref}$. In this way, the relevant case of balanced sinusoidal output voltages, corresponding to v_{2ref} = 0, v_{3ref} = 0, and v_{4ref} = 0, can be optimized.

The d_1-q_1 plane can be subdivided into 18 sectors with an angular size of π/9 for determining the eight active configurations, as shown in Fig. 2. Each sector identifies four active

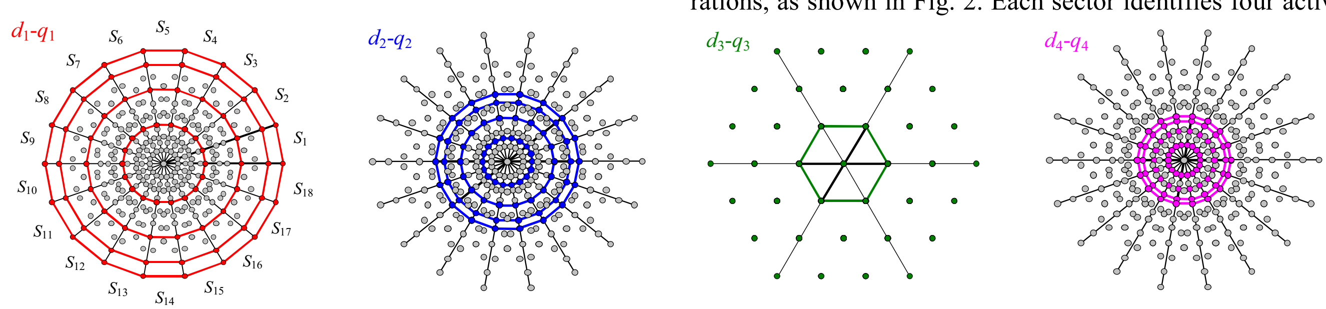

Fig. 2. Output voltage vectors corresponding to the inverter configurations in the four d-q planes.

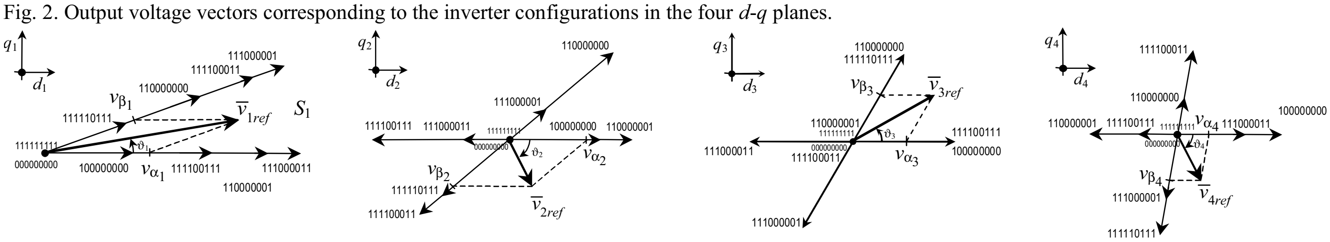

Fig. 3. Inverter configurations and corresponding load voltage vectors in the case of $\overline{v}_{1ref}$ lying in sector S_1.

configurations on its left border and four active configurations on its right border, as shown in Fig. 3 with reference to sector 1. These eight configurations are determined so that a switching pattern requiring a single commutation for each configuration change can be defined for each sector, starting from the null configuration (000000000) up to the other null configuration (111111111), as shown in Table I. The duty cycles corresponding to the switch configurations are indicated in the first column, from δ_0 up to δ_9. The second half of the switching period consists in following backward the switching pattern from (111111111) to (000000000).

There are ten magnitudes at all corresponding to the switch configurations involved in the switching pattern (i.e., V_A, V_B, V_C, V_D, V_E, V_F, V_G, V_H, V_I, V_L, in increasing order). They can be expressed on the basis of only four coefficients K_1, K_2, K_3, and K_4 as

$$\begin{cases} V_A = \frac{2}{9}\left(2\cos\frac{4\pi}{9}\right)V_{dc} = \frac{2}{9}\frac{K_1}{K_4}V_{dc} \cong 0.077V_{dc} \\ V_B = \frac{2}{9}\left(2\cos\frac{2\pi}{9}-1\right)V_{dc} = \frac{2}{9}\frac{K_1}{K_2}V_{dc} \cong 0.118V_{dc} \\ V_C = \frac{2}{9}\left(1-2\cos\frac{4\pi}{9}\right)V_{dc} = \frac{2}{9}\frac{K_2}{K_4}V_{dc} \cong 0.145V_{dc} \\ V_D = \frac{2}{9}\left(2\cos\frac{\pi}{9}-1\right)V_{dc} = \frac{2}{9}\frac{K_3}{K_4}V_{dc} \cong 0.195V_{dc} \\ V_E = \frac{2}{9}V_{dc} \cong 0.222V_{dc} \\ V_F = \frac{2}{9}\left(1+2\cos\frac{4\pi}{9}\right)V_{dc} = \frac{2}{9}\frac{K_3}{K_2}V_{dc} \cong 0.299V_{dc} \\ V_G = \frac{2}{9}\left(2\cos\frac{2\pi}{9}\right)V_{dc} = \frac{2}{9}\frac{K_4}{K_2}V_{dc} \cong 0.340V_{dc} \\ V_H = \frac{2}{9}\left(2\cos\frac{\pi}{9}\right)V_{dc} = \frac{2}{9}\frac{K_2}{K_1}V_{dc} \cong 0.418V_{dc} \\ V_I = \frac{2}{9}\left(1+2\cos\frac{2\pi}{9}\right)V_{dc} = \frac{2}{9}\frac{K_3}{K_1}V_{dc} \cong 0.563V_{dc} \\ V_L = \frac{2}{9}\left(1+2\cos\frac{\pi}{9}\right)V_{dc} = \frac{2}{9}\frac{K_4}{K_1}V_{dc} \cong 0.640V_{dc}, \end{cases} \tag{5}$$

being

$$\begin{cases} K_1 = \sin\frac{\pi}{9} \cong 0.342, \quad K_2 = \sin\frac{2\pi}{9} \cong 0.643 \\ K_3 = \sin\frac{3\pi}{9} \cong 0.866, \quad K_4 = \sin\frac{4\pi}{9} \cong 0.985. \end{cases}$$

Fig. 2 shows that the switch configurations utilized in the proposed modulation strategy correspond to load voltage vectors lying on vertexes of four 18-sided regular polygons having radii V_E, V_H, V_I, V_L, respectively, on the d_1-q_1 plane. Also in the d_2-q_2 and d_4-q_4 planes the load voltage vectors lie on vertexes of four 18-sided regular polygons having radii V_B, V_E, V_F, V_G, and V_A, V_C, V_D, V_E, respectively. Instead, in the d_3-q_3 plane, the load voltage vectors lie on vertexes of a single regular hexagon having radius V_E, leading to multiple vectors, both the active and the null ones.

In order to present the details of the proposed space vector modulation strategy, the case of $\overline{v}_{1ref}$ lying in sector S_1 is considered. Fig. 3 shows the inverter switch configurations and the corresponding output voltage vectors involved in the switching pattern in the d_1-q_1, d_2-q_2, d_3-q_3, and d_4-q_4 planes. For each reference space vector v_{href} (h = 1, 2, 3, 4) the two components $v_{\alpha h}$ and $v_{\beta h}$ along proper directions are defined, according to Fig. 3, leading to

$$\begin{cases} \overline{v}_{1ref} = v_{1ref}e^{j\vartheta_1} = \overline{v}_{\alpha_1} + \overline{v}_{\beta_1} = v_{\alpha_1} + v_{\beta_1}e^{j\frac{\pi}{9}} \\ \overline{v}_{2ref} = v_{2ref}e^{-j\vartheta_2} = \overline{v}_{\alpha_2} + \overline{v}_{\beta_2} = v_{\alpha_2} - v_{\beta_2}e^{j\frac{2\pi}{9}} \\ \overline{v}_{3ref} = v_{3ref}e^{j\vartheta_3} = \overline{v}_{\alpha_3} + \overline{v}_{\beta_3} = v_{\alpha_3} + v_{\beta_3}e^{j\frac{3\pi}{9}} \\ \overline{v}_{4ref} = v_{4ref}e^{-j\vartheta_4} = \overline{v}_{\alpha_4} + \overline{v}_{\beta_4} = v_{\alpha_4} - v_{\beta_4}e^{j\frac{4\pi}{9}} \end{cases}, \tag{6}$$

where

$$\begin{cases} v_{\alpha_1} = \frac{\sin(\pi/9-\vartheta_1)}{K_1}v_{1ref}, \quad v_{\beta_1} = \frac{\sin\vartheta_1}{K_1}v_{1ref} \\ v_{\alpha_2} = \frac{\sin(2\pi/9+\vartheta_2)}{K_2}v_{2ref}, \quad v_{\beta_2} = \frac{\sin\vartheta_2}{K_2}v_{2ref} \\ v_{\alpha_3} = \frac{\sin(3\pi/9-\vartheta_3)}{K_3}v_{3ref}, \quad v_{\beta_3} = \frac{\sin\vartheta_3}{K_3}v_{3ref} \\ v_{\alpha_4} = \frac{\sin(4\pi/9+\vartheta_4)}{K_4}v_{4ref}, \quad v_{\beta_4} = \frac{\sin\vartheta_4}{K_4}v_{4ref} \end{cases}. \tag{7}$$

Then, the reference components v_{α_h} and v_{β_h} can be synthesized as weighted average of the space vector magnitudes, over the switching period T, introducing the corresponding application times t_1, t_2, …, t_8, leading to

$$\begin{cases} v_{\alpha_1} = \frac{t_1}{T}V_E + \frac{t_3}{T}V_I + \frac{t_5}{T}V_L + \frac{t_7}{T}V_H \\ v_{\beta_1} = \frac{t_8}{T}V_E + \frac{t_6}{T}V_I + \frac{t_4}{T}V_L + \frac{t_2}{T}V_H \\ v_{\alpha_2} = \frac{t_1}{T}V_E + \frac{t_3}{T}V_F - \frac{t_5}{T}V_B - \frac{t_7}{T}V_G \\ v_{\beta_2} = \frac{t_8}{T}V_E + \frac{t_6}{T}V_F - \frac{t_4}{T}V_B - \frac{t_2}{T}V_G \\ v_{\alpha_3} = \frac{t_1}{T}V_E + \frac{t_3}{T}0 - \frac{t_5}{T}V_E + \frac{t_7}{T}V_E \\ v_{\beta_3} = \frac{t_8}{T}V_E + \frac{t_6}{T}0 - \frac{t_4}{T}V_E + \frac{t_2}{T}V_E \\ v_{\alpha_4} = \frac{t_1}{T}V_E - \frac{t_3}{T}V_D + \frac{t_5}{T}V_C - \frac{t_7}{T}V_A \\ v_{\beta_4} = \frac{t_8}{T}V_E - \frac{t_6}{T}V_D + \frac{t_4}{T}V_C - \frac{t_2}{T}V_A \end{cases} \tag{8}$$

The relationships (8) define a system of eight linear equations, assuming the application times of the active configurations t_1, t_2, …, t_8 as unknown variables.

The application times of the null configurations t_0 and t_9 can be determined as follows:

$$t_0 + t_9 = T - (t_1 + t_2 + t_3 + t_4 + t_5 + t_6 + t_7 + t_8). \tag{9}$$

It should be noted that (9) does not allow the determina-

TABLE I - SWITCHING TABLE OF THE PROPOSED SVM CONTROL STRATEGY FOR ALL THE 18 SECTORS ON PLANE d_1-q_1.

	1	2	3	4	5	6	7	8	9	10	11	12	13	14	15	16	17	18
δ_0	000000000	000000000	000000000	000000000	000000000	000000000	000000000	000000000	000000000	000000000	000000000	000000000	000000000	000000000	000000000	000000000	000000000	000000000
δ_1	100000000	010000000	010000000	001000000	001000000	000100000	000100000	000010000	000010000	000001000	000001000	000000100	000000100	000000010	000000010	000000001	000000001	100000000
δ_2	110000000	110000000	011000000	011000000	001100000	001100000	000110000	000110000	000011000	000011000	000001100	000001100	000000110	000000110	000000011	000000011	100000001	100000001
δ_3	110000001	111000000	111000000	011100000	011100000	001110000	001110000	000111000	000111000	000011100	000011100	000001110	000001110	000000111	000000111	100000011	100000011	110000001
δ_4	111000001	111000001	111100000	111100000	011110000	011110000	001111000	001111000	000111100	000111100	000011110	000011110	000001111	000001111	100000111	100000111	110000011	110000011
δ_5	111000011	111100001	111100001	111110000	111110000	011111000	011111000	001111100	001111100	000111110	000111110	000011111	000011111	100001111	100001111	110000111	110000111	111000011
δ_6	111100011	111100011	111110001	111110001	111111000	111111000	011111100	011111100	001111110	001111110	000111111	000111111	100011111	100011111	110001111	110001111	111000111	111000111
δ_7	111100111	111110011	111110011	111111001	111111001	111111100	111111100	011111110	011111110	001111111	001111111	100111111	100111111	110011111	110011111	111001111	111001111	111100111
δ_8	111110111	111110111	111111011	111111011	111111101	111111101	111111110	111111110	011111111	011111111	101111111	101111111	110111111	110111111	111011111	111011111	111101111	111101111
δ_9	111111111	111111111	111111111	111111111	111111111	111111111	111111111	111111111	111111111	111111111	111111111	111111111	111111111	111111111	111111111	111111111	111111111	111111111

tion of t_0 and t_9 separately, leading to a degree of freedom that can be utilized in order to modify the modulation properties in terms of switching frequency and output current distortion [12]. Introducing the duty-cycles δ_k, (9) can be rewritten as

$$\delta_0 + \delta_9 = 1 - \left(\delta_1 + \delta_2 + \delta_3 + \delta_4 + \delta_5 + \delta_6 + \delta_7 + \delta_8\right), \quad (10)$$

being

$$\delta_k = \frac{t_k}{T}, \; k = 0, 1, \ldots, 9. \quad (11)$$

The original linear system (8) can be decomposed into two independent systems of 4 equations with 4 unknowns, characterized by the same matrix of coefficients $[M]$, leading to

$$\frac{2}{9} V_{dc} [M] \begin{bmatrix} \delta_1 \\ \delta_3 \\ \delta_5 \\ \delta_7 \end{bmatrix} = \begin{bmatrix} v_{\alpha_1} \\ v_{\alpha_2} \\ v_{\alpha_3} \\ v_{\alpha_4} \end{bmatrix}, \quad \frac{2}{9} V_{dc} [M] \begin{bmatrix} \delta_8 \\ \delta_6 \\ \delta_4 \\ \delta_2 \end{bmatrix} = \begin{bmatrix} v_{\beta_1} \\ v_{\beta_2} \\ v_{\beta_3} \\ v_{\beta_4} \end{bmatrix}, \quad (12)$$

where

$$[M] = \begin{bmatrix} 1 & K_3/K_1 & K_4/K_1 & K_2/K_1 \\ 1 & K_3/K_2 & -K_1/K_2 & -K_4/K_2 \\ 1 & 0 & -1 & 1 \\ 1 & -K_3/K_4 & K_2/K_4 & -K_1/K_4 \end{bmatrix}. \quad (13)$$

Since the matrix $[M]$ is nonsingular ($det\ [M] = 27$), the system has the following unique solution:

$$\begin{bmatrix} \delta_1 \\ \delta_3 \\ \delta_5 \\ \delta_7 \end{bmatrix} = \frac{9}{2V_{dc}} [M]^{-1} \begin{bmatrix} v_{\alpha_1} \\ v_{\alpha_2} \\ v_{\alpha_3} \\ v_{\alpha_4} \end{bmatrix}, \quad \begin{bmatrix} \delta_8 \\ \delta_6 \\ \delta_4 \\ \delta_2 \end{bmatrix} = \frac{9}{2V_{dc}} [M]^{-1} \begin{bmatrix} v_{\beta_1} \\ v_{\beta_2} \\ v_{\beta_3} \\ v_{\beta_4} \end{bmatrix}, \quad (14)$$

where

$$[M]^{-1} = \frac{4}{9} \begin{bmatrix} K_1^2 & K_2^2 & K_3^2 & K_4^2 \\ K_1 K_3 & K_3 K_2 & 0 & -K_4 K_3 \\ K_1 K_4 & -K_1 K_2 & -K_3^2 & K_2 K_4 \\ K_1 K_2 & -K_2 K_4 & K_3^2 & -K_1 K_4 \end{bmatrix}. \quad (15)$$

Introducing (7) in (14) the duty cycles of the proposed space vector modulation strategy are obtained on the basis of the reference space vectors, as follows

$$\begin{cases} \begin{bmatrix} \delta_1 \\ \delta_3 \\ \delta_5 \\ \delta_7 \end{bmatrix} = \dfrac{2}{V_{dc}} \begin{bmatrix} K_1 & K_2 & K_3 & K_4 \\ K_3 & K_3 & 0 & -K_3 \\ K_4 & -K_1 & -K_3 & K_2 \\ K_2 & -K_4 & K_3 & -K_1 \end{bmatrix} \begin{bmatrix} \sin(\pi/9 - \vartheta_1) v_{1ref} \\ \sin(2\pi/9 + \vartheta_2) v_{2ref} \\ \sin(3\pi/9 - \vartheta_3) v_{3ref} \\ \sin(4\pi/9 + \vartheta_4) v_{4ref} \end{bmatrix} \\ \begin{bmatrix} \delta_8 \\ \delta_6 \\ \delta_4 \\ \delta_2 \end{bmatrix} = \dfrac{2}{V_{dc}} \begin{bmatrix} K_1 & K_2 & K_3 & K_4 \\ K_3 & K_3 & 0 & -K_3 \\ K_4 & -K_1 & -K_3 & K_2 \\ K_2 & -K_4 & K_3 & -K_1 \end{bmatrix} \begin{bmatrix} \sin \vartheta_1 v_{1ref} \\ \sin \vartheta_2 v_{2ref} \\ \sin \vartheta_3 v_{3ref} \\ \sin \vartheta_4 v_{4ref} \end{bmatrix} \end{cases}. \quad (16)$$

Note that a null coefficient appears in (15) and (16) since the switch configurations corresponding to δ_3 and δ_6 (i.e., the ones having three and six adjacent 1, respectively) represent a null vector in the d_3-q_3 plane. Then, both δ_3 and δ_6 are not affected by $\bar{v}_{3ref}$.

In the particular case of $v_{2ref} = 0$, $v_{3ref} = 0$, and $v_{4ref} = 0$, (16) assumes the following simplified form:

$$\begin{cases} \delta_1 = \left(\dfrac{2}{V_{dc}} K_1^2\right) v_{\alpha_1} \\ \delta_3 = \left(\dfrac{2}{V_{dc}} K_1 K_3\right) v_{\alpha_1} \\ \delta_5 = \left(\dfrac{2}{V_{dc}} K_1 K_4\right) v_{\alpha_1} \\ \delta_7 = \left(\dfrac{2}{V_{dc}} K_1 K_2\right) v_{\alpha_1} \end{cases} \quad \begin{cases} \delta_8 = \left(\dfrac{2}{V_{dc}} K_1^2\right) v_{\beta_1} \\ \delta_6 = \left(\dfrac{2}{V_{dc}} K_1 K_3\right) v_{\beta_1} \\ \delta_4 = \left(\dfrac{2}{V_{dc}} K_1 K_4\right) v_{\beta_1} \\ \delta_2 = \left(\dfrac{2}{V_{dc}} K_1 K_2\right) v_{\beta_1} \end{cases}. \quad (17)$$

Introducing the coefficient $K = 9K_1^2 / V_{dc}^2$ the previous relationships can be rewritten as

$$\begin{cases} \delta_1 = K\, V_E\, v_{\alpha_1} \\ \delta_3 = K\, V_I\, v_{\alpha_1} \\ \delta_5 = K\, V_L\, v_{\alpha_1} \\ \delta_7 = K\, V_H\, v_{\alpha_1} \end{cases} \quad \begin{cases} \delta_8 = K\, V_E\, v_{\beta_1} \\ \delta_6 = K\, V_I\, v_{\beta_1} \\ \delta_4 = K\, V_L\, v_{\beta_1} \\ \delta_2 = K\, V_H\, v_{\beta_1} \end{cases}. \quad (18)$$

It can be noted that the duty cycle of each active configuration is proportional to the magnitude of the corresponding voltage vector on d_1-q_1 [8], [10].

V. MAXIMUM MODULATION INDEX

The modulation index m is defined as the ratio between the amplitude of the line-to-neutral voltage and the dc-link voltage, in balanced sinusoidal operating conditions. In this case, the voltage amplitude of all phases coincides with the magnitude v_1 of the space vector lying on d_1-q_1 plane. Then,

$$m = v_1 / V_{dc} \,. \tag{19}$$

In order to determine the maximum value of the modulation index, the modulation constraints are introduced. In particular, the application times of active and null configurations involved in the switching pattern must be non-negative. These conditions can be written in terms of duty cycles as

$$\delta_k \geq 0 \,,\; k = 0, 1, \ldots, 9. \tag{20}$$

In the case of $v_{2ref} = 0$, $v_{3ref} = 0$ and $v_{4ref} = 0$, as for balanced sinusoidal voltages, the duty cycles corresponding to the active configurations are always non-negative. In fact, all the terms in (17) are non-negative. In this case, the modulation constraints are represented only by the following inequalities

$$\delta_0 \geq 0 \,,\; \delta_9 \geq 0. \tag{21}$$

Introducing (21) in (10) yields

$$\delta_1 + \delta_2 + \delta_3 + \delta_4 + \delta_5 + \delta_6 + \delta_7 + \delta_8 \leq 1. \tag{22}$$

Then, combining (22) with the expression of the duty cycles (17) leads to

$$v_{\alpha_1} + v_{\beta_1} \leq \frac{V_{dc}}{2K_4^2} \,. \tag{23}$$

This condition is satisfied by voltage space vectors lying within the triangle defined by the space vectors $V_{dc}/(2K_4^2)$ and $V_{dc}/(2K_4^2)\, e^{j\pi/9}$ on the d_1-q_1 plane. By extending this procedure to all the 18 sectors on d_1-q_1 plane the 18-sided regular polygon shown in Fig. 4 is obtained. Then, $\overline{v}_{1ref}$ is confined inside this polygon.

If balanced sinusoidal line-to-neutral voltages are required $\overline{v}_{1ref}$ lies on a circle. In this case the maximum voltage amplitude corresponds to the radius of the circle inscribed in the limit polygon. As a consequence, the modulation index is

$$m \leq \frac{1}{2K_4^2} \cos(\pi/18) = \frac{1}{2\cos(\pi/18)} \cong 0.508 \,. \tag{24}$$

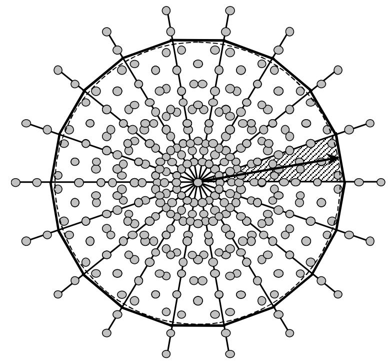

Fig. 4. Regular polygon in d_1-q_1 plane representing the limit of $\overline{v}_{1ref}$.

It can be noted that this limit coincides with the theoretical limit given in [3] for a multi-phase VSI with sinusoidal balanced output voltages ($n = 9$)

$$m \leq \frac{1}{2\sin\left[\frac{\pi}{2}\left(\frac{n-1}{n}\right)\right]} = \frac{1}{2\cos(\pi/2n)} \,. \tag{25}$$

VI. Simulation Results

In order to verify the effectiveness of the proposed SVM strategy, the behavior of a system, composed by a nine-phase VSI feeding a nine-phase balanced R-L load has been tested by numerical simulations ($R = 20\ \Omega$, $L = 10$ mH, $V_{dc} = 540$ V, see Fig. 1). The numerical results are obtained in balanced and sinusoidal conditions, with an amplitude of the reference load voltage $|\overline{v}_{1ref}| = 200$ V and a frequency of 50 Hz.

The choice $\delta_0 = \delta_9$ has been considered for the null configurations in each cycle ($T = 200$ µs). The resulting SVM strategy can be considered as an extension of the well-known "symmetrical SVM" utilized for the three-phase VSI.

The nine load currents are shown in Fig. 5. Note that the waveforms are practically sinusoidal and characterized by a small ripple due to the switching effect.

The line-to-neutral load voltage v_1 is represented in Fig. 6, showing a 17-levels waveform: $0, \pm\frac{1}{9}V_{dc}, \pm\frac{2}{9}V_{dc}, \ldots, \pm\frac{8}{9}V_{dc}$.

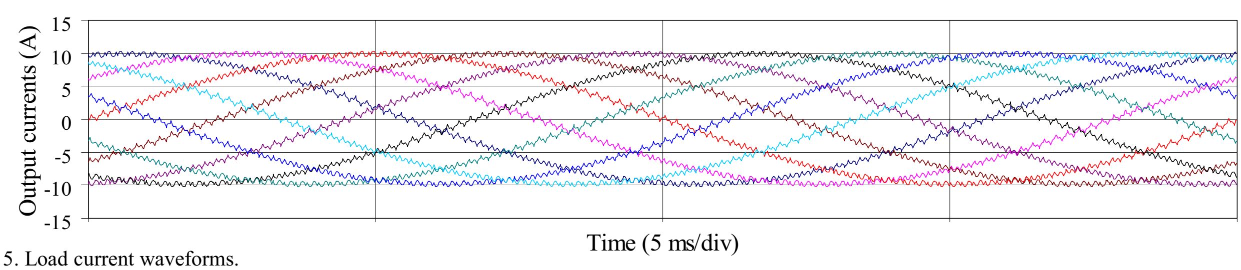

Fig. 5. Load current waveforms.

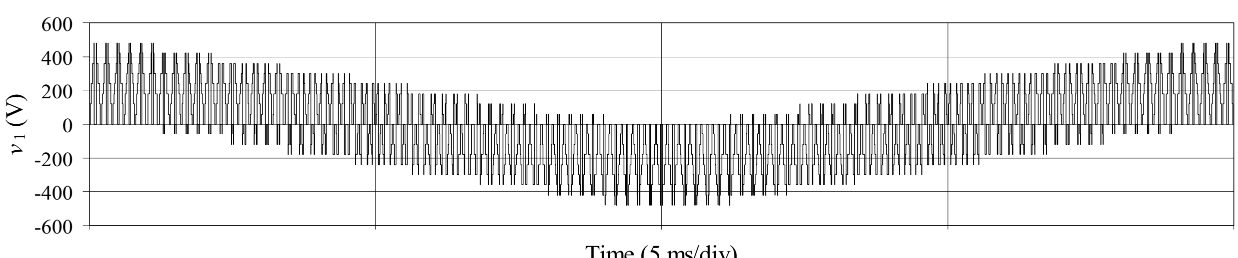

Fig. 6. Line-to-neutral load voltage waveform (v_1).

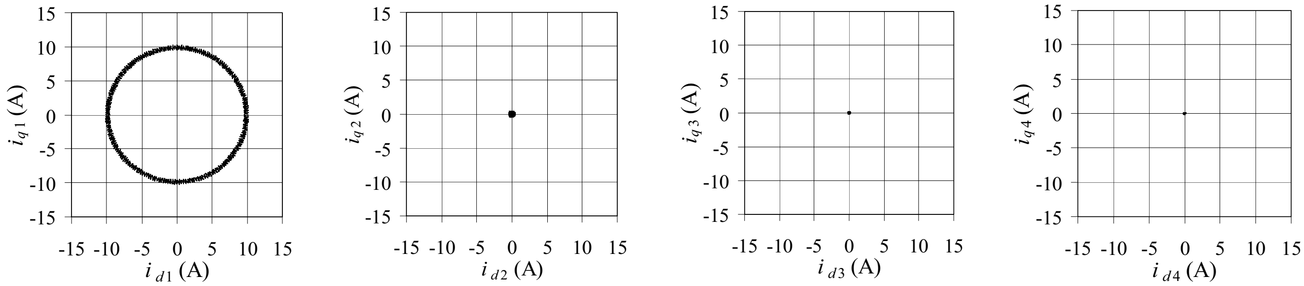

Fig. 7. Trajectories of space vectors $\bar{i}_1$, $\bar{i}_2$, $\bar{i}_3$, and $\bar{i}_4$ in the corresponding *d-q* planes.

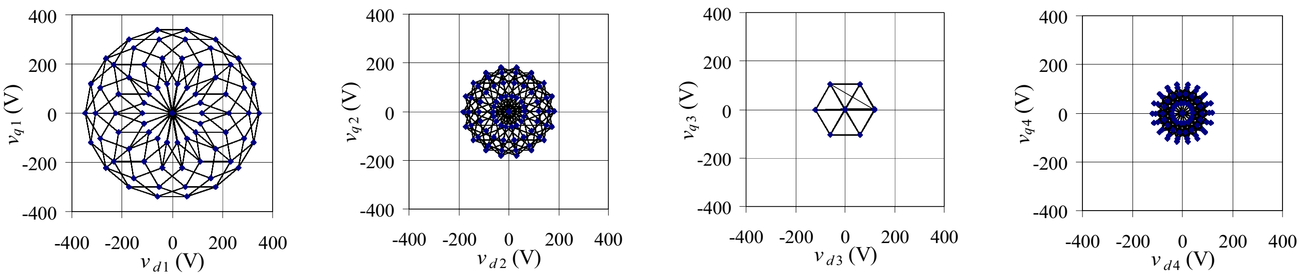

Fig. 8. Loci of space vectors $\bar{v}_1$, $\bar{v}_2$, $\bar{v}_3$, and $\bar{v}_4$ in the corresponding *d-q* planes.

In particular, the instantaneous value of v_1 changes across nine adjacent levels in a voltage range of $\frac{8}{9}V_{dc}$ within each cycle period, as expressed by (4).

In Fig. 7 are illustrated the trajectories of the space vectors $\bar{i}_1$, $\bar{i}_2$, $\bar{i}_3$, and $\bar{i}_4$ in the corresponding *d-q* planes. As expected, the space vectors $\bar{i}_2$, $\bar{i}_3$, and $\bar{i}_4$ are practically null, whereas $\bar{i}_1$ moves along a circular trajectory (at constant speed). These results demonstrate that the proposed SVM strategy is able to independently control the output voltage space vectors in the four different *d-q* planes.

In Fig. 8 the loci of space vectors $\bar{v}_1$, $\bar{v}_2$, $\bar{v}_3$, and $\bar{v}_4$, are shown in the corresponding *d-q* planes. In this figure the dots represent voltage space vectors involved in the modulation process, whereas the lines connect successive configurations.

VII. Conclusion

A SVM control strategy for nine-phase VSI has been proposed in this paper as an extension of the SVM already developed for 5- and 7-phase VSIs. The modulation is based on multiple space vector approach applied to nine-phase circuits, leading to quadruple *d-q* planes representation.

The switching pattern includes eight active and two null configurations, with a single leg commutation for each configuration change. The duty cycles of both active and null inverter configurations are calculated on the basis of a detailed space vector approach, leading to the analytical determination of the modulation limits.

The results obtained by the proposed modulation strategy collapse in the ones obtainable with a carrier-based symmetrical PWM in the case of $v_{2ref} = 0$, $v_{3ref} = 0$, and $v_{4ref} = 0$, as for balanced sinusoidal voltages. In this case, it has been verified that the modulation limits are in agreement with the theoretical maximum modulation index of a nine-phase VSI, proving that the proposed SVM allows full dc bus voltage utilization.

Numerical simulations carried out with reference to a nine-phase VSI supplying a nine-phase balanced load confirm the effectiveness of the proposed SVM strategy.

References

[1] H.A. Toliyat, S.P. Waikar, T.A. Lipo, "Analysis and simulation of five-phase synchronous reluctance machines including third harmonic of airgap MMF," *IEEE Trans. on Industry Applications*, vol. 34, no. 2, March/April 1998, pp. 332-339.

[2] H. Xu, H.A. Toliyat, L.J. Petersen, "Five-phase induction motor drives with DSP-based control system," *IEEE Trans. on Power Electronics*, vol. 17, No. 4, July 2002, pp. 524-533.

[3] D. Casadei, G. Serra, A. Tani, L. Zarri, "Multi-phase inverter modulation strategies based on duty-cycle space vector approach," *Proc. of Ship Propulsion and Railway Systems Conference (SPRTS)*, Bologna (Italy), 4-6 October 2005, pp. 222-229.

[4] A. Iqbal, E. Levi, M. Jones, S. N. Vukosavic, "A PWM scheme for a five-phase vsi supplying a five-phase two-motor drive," *Proc. of IECON Conference*, Paris (F), November 7-10, 2006, pp. 2575-2580.

[5] P.S.N. de Silva, J.E. Fletcher, B.W. Williams, "Development of space vector modulation strategies for five phase voltage source inverters," *Proc. of Power Electronics, Machines and Drives Conference (PEMD)*, March 31 – April 2, 2004, Vol. 2, pp. 650-655.

[6] A. Iqbal, E. Levi, "Space vector modulation schemes for a five-phase voltage source inverter," *Proc. of European Power Electronic Conference, EPE*, Sept. 11-14, 2005, Dresden (D), pp. 1-12.

[7] H.M. Ryu, J.W. Kim, S.K. Sul, "Analysis of multi-phase space vector pulse width modulation based on multiple d-q spaces concept," *IEEE Trans. on Power Electronics*, Vol. 20, No. 6, Nov. 2005. pp. 1364-1371.

[8] G. Grandi, G. Serra, A. Tani, "Space vector modulation of a seven-phase voltage source inverter," *Symposium on Power Electronics, Electrical Drives and Advanced Electrical Motors*, *SPEEDAM*, Taormina (IT), May 23-26, 2006.

[9] G. Grandi, G. Serra, A. Tani, "General analysis of multi-phase systems based on space vector approach," *Proc. of 12th Power Electronics and Motion Control Conference (EPE-PEMC)*, Portoroz (Slovenia), Aug. 30 - Sept. 1, 2006.

[10] J.W. Kelly, E.G. Strangas, J.M. Miller, "Multiphase space vector Pulse Width Modulation," *IEEE Trans. on Energy Conversion*, vol. 18, no. 2, pp. 259-264, June 2003.

[11] M.J. Duran, E. Levi, M. Jones, "Independent vector control of asymmetrical nine-phase machines by means of series connection," *Proc. of Electric Machines and Drives Conference*, *IEEE-EMD*, 15-18 May 2005, pp. 167 – 173.

[12] D. Casadei, G. Serra, A. Tani and L. Zarri, "Theoretical and experimental analysis for the RMS current ripple minimization in induction motor drives controlled by SVM technique," *IEEE Trans. on Industrial Electronics*, Vol. 51, No. 5, pp. 1056-1065, Nov. 2004.